Orchard Central, Singapore

Fellenius, B.H., and Tan, S.A., 2010. Combination of bidirectional-cell test and conventional head-down test. The Art of Foundation Engineering Practice, ""Honoring Clyde Baker", ASCE Geotechnical Special Publication, Edited by M.H. Hussein, J.B. Anderson, and W.M. Camp, GSP 198, pp. 240-259.

Combination of bidirectional-cell test and conventional head-down test

Bengt H. Fellenius[1)], M.ASCE and Tan Siew Ann[2)], M.ASCE

[1)] 2475 Rothesay Avenue, Sidney, British Columbia, V8L 2B9. <Bengt@Fellenius.net>

[2)] Civil Engineering Department, National University of Singapore, 10 Kent Ridge Crescent, Singapore 119260. <cvetansa@nus.edu.sg>

ABSTRACT. Bidirectional-cell tests were performed in Singapore on four bored piles in a residual soil and underlying weathered, highly fractured bedrock called the Bukit Timah Granite formation. Two of the piles were 1.2 m diameter, uninstrumented, and 28 m and 38 m long. The other two were strain-gage instrumented, 1.0 m diameter piles, both 37 m long. The latter tests combined the cell test with conventional head-down testing. Analysis of the test results indicated that the pile toe stiffness was low. The evaluation of the strain-gage data showed that the pile material modulus was a function of the induced strain. The desired axial working load was 10 MN, and the combined cell and head-down tests correlated to a head-down test with a maximum applied load of 38 MN, which, although smaller than the ultimate resistance of the piles, was taken as the capacity of piles constructed similar to the second set of test piles at the site.

KEYWORDS Bored piles, bidirectional-cell tests, load-distribution, load-movement, residual soil, weathered granite, strain-gage analysis, modulus evaluation, CPTU correlation.

1. INTRODUCTION

In validating the design for a new shopping center complex at Orchard Central, Singapore, static loading tests (proof tests) were performed on two 1.2 m diameter bored piles, constructed to depths of 28 m (Pile C54a) and 38 m (Pile C57). Both pile toes were located in weathered granite bedrock (see description below). Based on information from boreholes drilled close to the piles; Pile C54a was socketed about 6.3 m into the granite bedrock, and Pile C57 was just seated onto the bedrock. Because the intent of the static loading tests was proof-testing, no strain-gage instrumentation was included. Both loading tests were with a single bidirectional-cell (Osterberg 1998; Fellenius 2000) placed at levels where the expected upper soil resistance would balance the lower resistance. The chosen cell depths were 24.0 m and 30.4 m, and the distances between the cell and the pile toe were 3.7 m

and 7.2 m, respectively. Fig. 1 shows the recorded upward and downward load-movements of the cell plates in the two tests. The downward load-movement curves indicate similar downward stiffness for the two piles despite the different lengths, while stiffness of the upward curves differs. The shaft resistance for the shorter pile is mostly in the weathered soil. For the longer pile, a sizeable portion is obtained in the weathered rock, which is why the upward stiffness for the shorter pile (Pile C54a) is much smaller than for the longer pile (Pile C57).

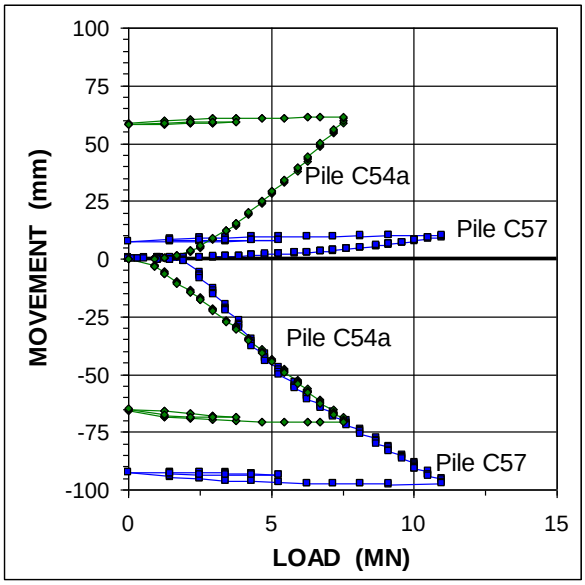

Fig. 1 Results of bidirectional-cell tests on two 1.2 m diameter bored piles installed to depths of 28 m (C54a) and 38 m (C57) at the site.

In contrast to a conventional head-down test, which only supplies the load applied to the pile head, a bidirectional-cell test establishes the load in two locations in the tested pile, as indicated in Fig. 2 for the maximum load applied in the tests. The shaft resistance distributions illustrated by the dashed straight lines infer that the mobilized shaft resistance is similar for the two piles. A potential shaft resistance distribution curve, proportional to effective stress applicable to both tests is also indicated in the figure. Assuming that the shaft resistance below the cell levels follows the same curved shape as above the cell levels establishes approximate toe resistance values for the tests, which suggest that the pile toe stiffness is rather small.

As is the requirement in Singapore, the acceptance criterion for the proof tests was a maximum pile head movement of 25 mm in the test at a load of 20 MN applied to the pile head, which load is twice the 10-MN desired allowable sustained axial design load for the piles, corresponding to maximum stress of about 8.5 MPa for a 1.2 m diameter bored pile. The acceptance criterion applies to a head-down test, which requires that the cell test be converted to a load-movement curve for an equivalent head-down test. This is produced by plotting a load-movement curve from adding the cell loads at equal movements and considering the larger pile shortening occurring in a head-down test as opposed to that found in a bidirectional-cell test (Fellenius 2009).

Fig. 3 shows the equivalent head-down load-movement curves determined from the cell test results for the two tests. Both curves fail the criterion as they plot well below the acceptance value. As indicated by the offset lines, the acceptance criterion is very close to the offset limit load for the two piles, commonly applied in North American practice. It is probable that had the toe response been stiffer, at least the longer pile, Pile C57, would have satisfied the criterion.

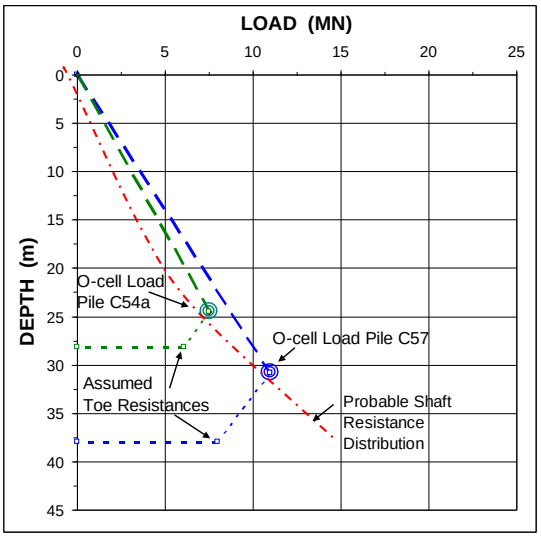

Fig. 2 Load-distribution curves.

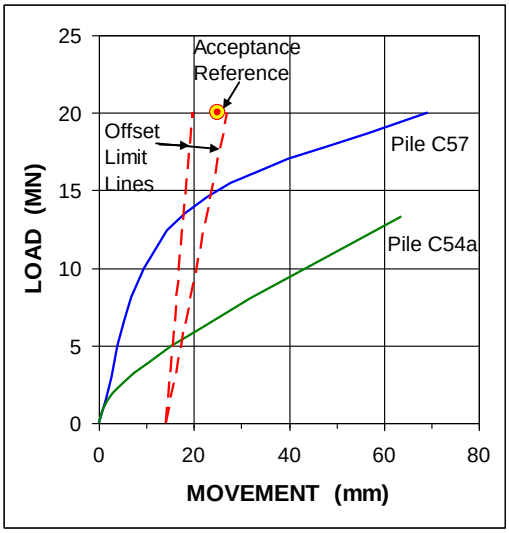

Fig. 3 The equivalent head-down load-movement curves

To resolve the issue, two new test piles, UTP-3 and UTP-4, were constructed. The new piles were instrumented with 12 levels of vibrating-wire strain-gage pairs to assess distribution shaft and toe resistances of the test piles. The construction procedure was similar to that for the previous piles. Special care was taken in the final cleaning, however.

The testing programme was changed to a combination of conventional head-down and bidirectional-cell tests, by first performing a head-down test and, subsequently, a bidirectional-cell test. In each pile, the cell assembly was placed just above the pile toe.

The objective of the new tests was to determine the pile toe stiffness and the shaft resistance distribution for 1.0 m diameter at the site in order to design the necessary pile length for similar size construction piles.

2. GEOLOGY AND SOIL PROFILE

The soil at the site consists of a surficial fill composed of construction debris, broken pieces of concrete, and clay on a deposit of residual soil of the Bukit Timah Granite formation, a saprolite, made up of clay, silt, and silty sand as a matrix within rock fragments and occasional boulders. Figure 4 presents the results of two CPTU soundings at the site pushed in a hole prebored to 3.5 m depth through the fill. To about 11 m depth at the CPTU sounding location, the soil profile is characterized by frequent layers of loose silt and sand of the Kallang fluvial deposits. The natural water content ranges from about 30 % through about 40 %. The groundwater table is located at a depth of about 4 m below the ground surface.

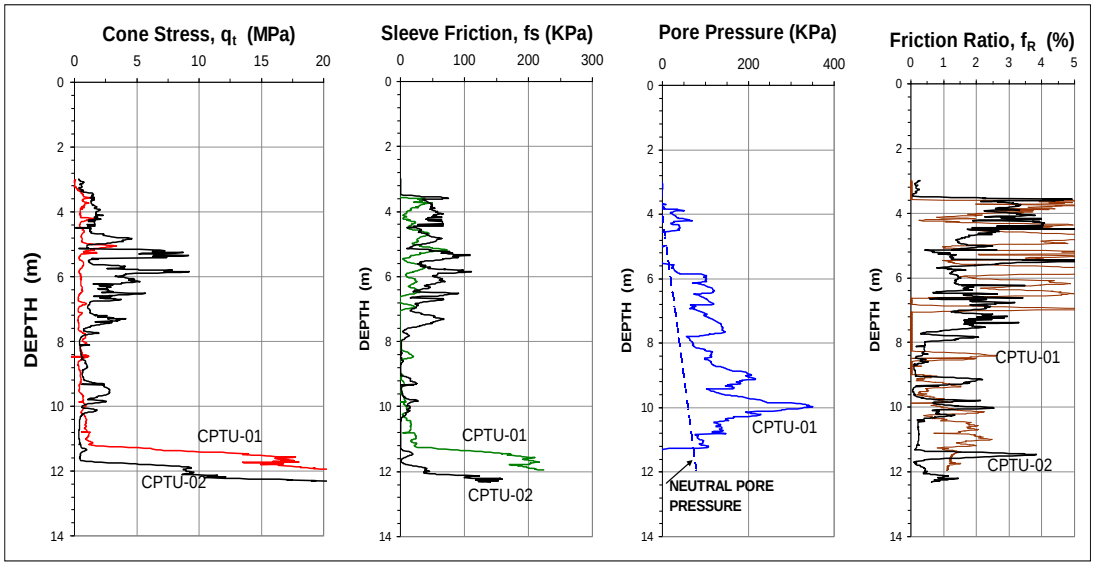

Fig. 4 Results of two CPTU soundings at the site. CPTU-01 and CPTU-02 close to test piles UTP-3 and UTP-4, respectively.

Figure 5 shows the soil profile determined from two bore holes, BH-2 and BH-3, about 30 m apart. The subject test piles, Piles UTP-3 and UTP-4, were constructed close to BH-2 and BH-3, respectively. As indicated, residual soil of the completely weathered Bukit Timah Granite formation is encountered at 11 m to 14 m depth. It is composed mainly of hard clayey silts, but also includes occasional layers of very dense silty fine sands.

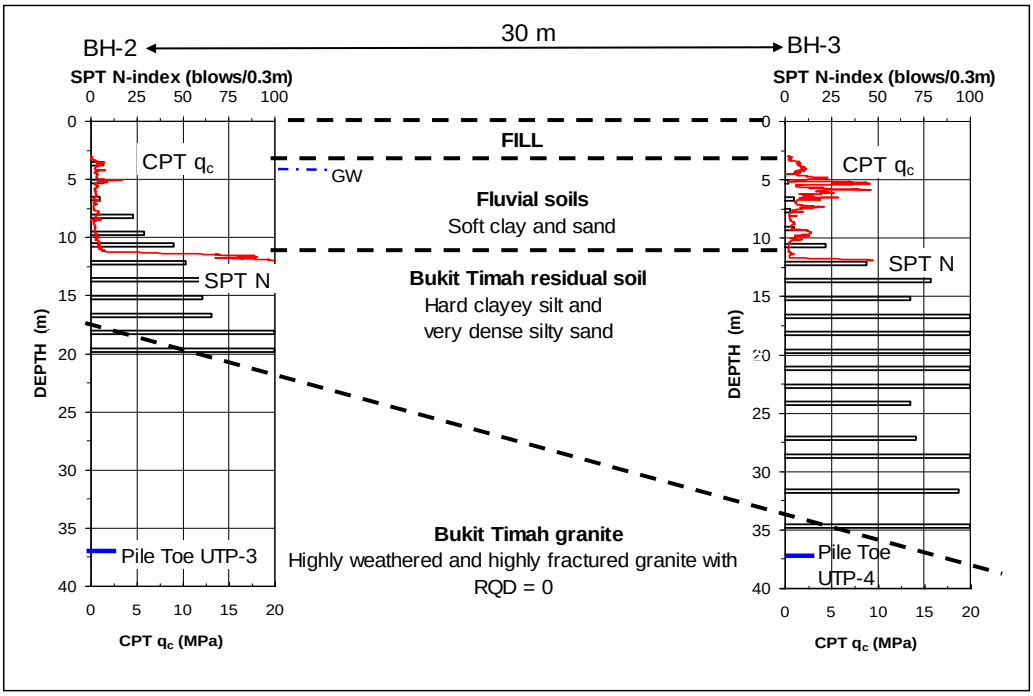

Fig. 5 Soil Profile at the two test piles.

At a depth of 20 m in BH-2 and 34 m in BH-3, the profile changes to bedrock consisting of a moderately to highly weathered and highly fractured Bukit Timah granite with a RQD of zero. Layers or zones of fine sand and silt were sporadically encountered in the boreholes. The drilling was terminated at 43 m depth about 6 m below the test pile depth.

Field observations and geophysical surveys show that due to the humid tropical condition in Singapore with high annual precipitation, the Bukit Timah granite has been weathered up to 70 m depth in some places. The main mechanism of weathering is chemical decomposition. The weathered Bukit Timah granite usually displays a sharp boundary between the residual soil and the weathered, highly fractured rock (Zao et al. 1994).

3. PILE CONSTRUCTION, PILE DATA, AND TEST ARRANGEMENT

The two test piles (1.0 m diameter), Piles UTP-3 (37.3 m deep) and UTP-4 (38.3 m deep), were drilled at the site, on May 31 and June 7, 2007, respectively. Below a 1.03 m O.D. temporary casing installed to a depth of 10 m, the pile shaft was uncased. The holes were kept open by means of bentonite slurry up to the bottom level of the casing. After the soil and debris had been carefully removed from the shaft using a cleaning bucket, concrete was placed by tremie from the bottom of the shaft (37 m depth) to the level of the intended lower end of the cell assembly, whereupon the reinforcing cage equipped with a cell assembly was inserted into the hole. Concrete was then placed by tremie into the pile until it reached prescribed level for the pile head 0.5 m above the ground surface. The temporary casing was withdrawn as the concrete level rose in the shaft. Final clean-out and concreting took place on May 31 and June 8, 2007, same day and one day after end of drilling, respectively. Also the final cleaning was performed with conventional mechanical cleaning buckets, used commonly in Singapore practice.

The cell assembly consisted of four 320 mm cells, each calibrated to its maximum capacity of 13.5 MN. The cell assemblies were placed at depths of 35.3 m and 36.3 m in the UTP-3 and UTP-4 test piles, 2 m above the pile toe depth, respectively.

The load from the bidirectional-cell is obtained by means of hydraulic pressure from a pump at the ground surface using water as fluid. The load acts in two opposing directions, resisted by the shaft resistance of the pile above and combined shaft and toe resistance below. Theoretically, the bidirectional-cell does not impose an additional upward load in the pile until its expansion force exceeds the buoyant weight of the pile above the cell plus any residual load being present. The cell load minus the buoyant weight of the pile above is defined as the net load in the pile. For the test piles, the buoyant weights above the lower cells were 0.44 MN and 0.46 MN, respectively.

Both test piles were prepared with two pairs of vibrating wire strain gages attached to the reinforcing cage 0.5 m below each cell assembly (lower plate level). Each pair consisted of two diametrically opposed vibrating wire sister bar gages Type Geokon Model 4150. Above the cell level, both piles had single pairs of vibrating wire gages placed at 33.75 m depth and then at every 2.5 m up along the pile shaft until 11.25 m depth, i.e. at ten gage levels. Two additional gage pairs were placed at 6.25 m and 1.75 m depth.

In each test pile, the pile instrumentation included three telltale rod extensometers between the cell bottom steel bearing plate to directly measure cell expansion and compression, and two telltales rods extending from the upper cell plate to the pile head to measure pile shortening and lengthening, as monitored by Linear Voltage Displacement Transducers (LVDTs) at the pile head. Two LVDTs attached to a reference system monitored the movement of the pile head. Two lengths of galvanized iron pipe were also installed, extending from the pile head to the cell in order to vent the gap in the pile that develops when expanding the cell.

A 28-MN kentledge reaction system served as reaction in the head-down test. The jack placed on the pile head and used in the head-down test was a 35-MN capacity cell with a 160-mm travel. A digital survey level (Leica NA3003) was also used to independently monitor the pile head movement.

All instrumentation was connected to a data logger (Data Electronics 615 GeoLogger) and the test data were recorded and stored automatically at 60-second intervals throughout both tests.

4. TEST PROGRAMME

The test programme comprised four stages for each pile.

- Stage 1: Loading pile head in increments of 1,000 KN applied every 10 minutes until reaching either the maximum capacity (pressure limit), travel of the jack, or the capacity of the pile, and then to unload the pile in increments of 2,000 KN every 5 minutes. The purpose of this stage was to test the pile in the conventional head-down manner.
- Stage 2: Activating the bidirectional-cell in increments of 800 KN every 10 minutes until reaching either the maximum capacity, or travel of the bidirectional-cell, or the upward or downward capacity of the pile. The purpose of this stage was to determine separately shaft resistance and pile toe response to load. It was not expected that the pile shaft resistance would provide smaller resistance than the pile toe. The purpose was also to prepare for Stage 3 by separating the cell plates.
- Stage 3: Repeat of Stage 1, but with the cell open and free draining, that is, the pile would function like a pure shaft-bearing pile free of toe resistance.
- Stage 4: Repeat Stage 2. The purpose of this stage was to provide reference to the evaluations of shaft resistance in Stages 1 through 3.

5. TEST RESULTS — LOAD-MOVEMENT

5.1 Pile UTP-3

5.12 Stages 1a and 1b (Head-down Test)

The UTP-3 test started 21 days after construction, by reading of all gages before applying load. These readings were then the reference ("zero") readings for the instrumentation throughout the test. Load was then applied to the pile head in 12 load increments to a gross load of 12.1 MN, when the loading had to be halted due to excessive upward movement of the main test beam. The pile was then unloaded in six decrements. The pile head movement at the maximum load was 13.6 mm, and upward deflection of the main beam was 101 mm.

The test was restarted after minimizing the space to the main beam of the kentledge system. (It would have been desirable to remove all kentledge weights, exchange the main beam with a stiffer arrangement, and replace the kentledge, but, because of time and costs, this was not possible). Load was now applied to the pile head in 15 increments until a maximum load of 19.5 MN, when, again, the loading had to be halted due to the excessive upward movement of the main test beam. The pile was then unloaded in ten decrements. The pile head movement at the maximum load was 27.7 mm, and the upward deflection of the main beam was 103 mm. A small pile toe movement was observed at the maximum load.

5.13 Stage 2 (bidirectional-cell Test)

After unloading the pile, the lower cell assembly was first pressurized in order to break the tack welds holding it closed (for handling and for placement in the pile) and to form the fracture plane in the concrete surrounding the base of the lower cells. The break itself does not need much force, but the break cannot occur before the force has become equal to the load locked in the pile due to the buoyant weight of the pile and any residual load. For Stage 2, the force would also have to overcome the additional load built in due to the load transfer in previous test stage. This break required a 2.17 MN force and a 0.2 mm bidirectional-cell expansion.

The bidirectional-cell assembly was then pressurized in 10 increments to a maximum cell load of 8.0 MN, which resulted in total and after unloading (net) downward movements of 20.6 mm and 18.6 mm, respectively, and total and after unloading (net) upward movements of 3.9 mm and 0.5 mm. No pile head movement occurred during Stage 2. The cell assembly was depressurized in five decrements.

5.14 Stage 3 (Head-down Test)

After unloading the cell and leaving it open and free to drain, the pile was again subjected to a head-down test. Load was applied to the pile head in 18 load increments to a total load of 17.9 MN, when, again, the loading had to be halted due to the excessive upward movement of the main test beam. The pile was then unloaded in nine decrements. The total pile head movement at the maximum load was 22.9 mm, and the upward deflection of the main beam was 125 mm. The downward total movement of the upper cell plate during Stage 3 for the maximum load was 2.7 mm, indicating that the shaft resistance along the lower length of the pile was engaged, but not fully mobilized.

5.15 Stage 4 (bidirectional-cell Test)

For Stage 4, the cell assembly was pressurized in 10 increments to a total bidirectional-cell load of 13.5 MN, which resulted in a 21.6 mm downward movement for the applied maximum load. Total downward movement was 40.2 mm. The upward movement for the maximum load was 4.6 mm. Total upward movement of the upper cell plate was 7.0 mm. The cell assembly was then depressurized in a single step.

Figures 6 and 7 present the load-movement curves of the test stages from head-down tests on Pile UTP-3, Stages 1 and 3 and bidirectional-cell tests of Stages 2 and 4. For comparison, the downward load-movement from Pile C57

bidirectional-cell test is added to Fig. 7. Pile UTP-3 and Pile C57 were constructed to the same depth, 38 m, but have different diameter, 1.0 m an and 1.2 m, respectively. If the curves would have been plotted for nominal stress instead of load, the difference in toe stiffness between the piles would have been even more pronounced.

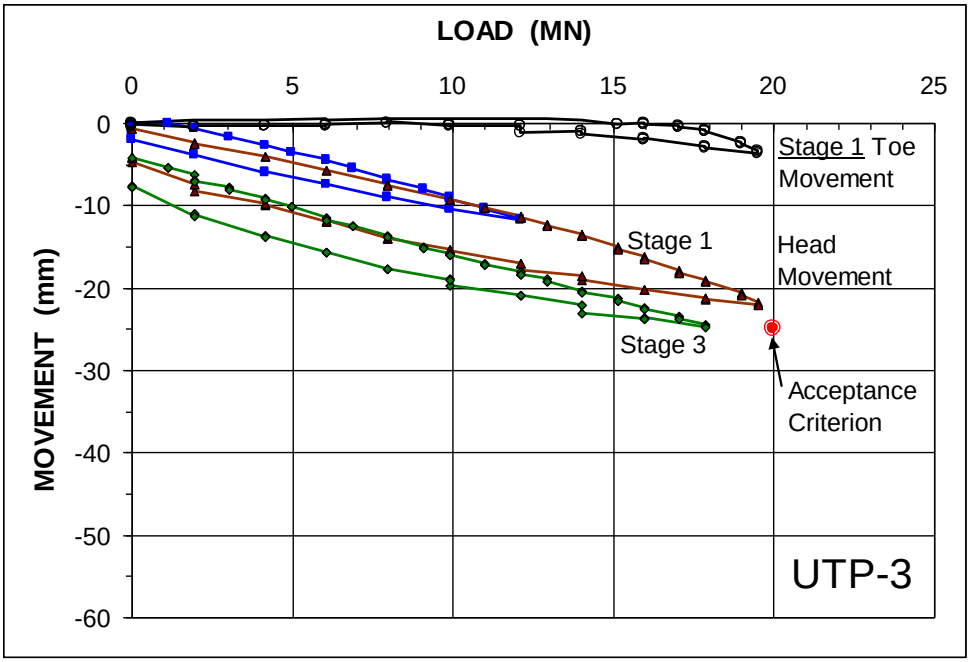

Fig. 6 Pile-head load-movement curves from Pile UTP-3; Stages 1 and 3.

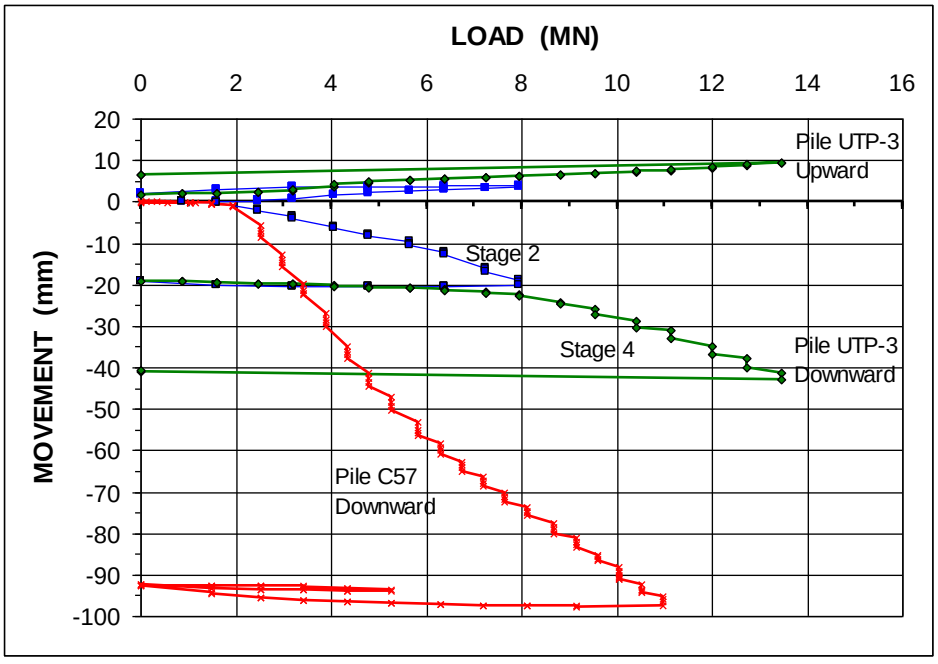

Fig. 7 Load-movement curves from Pile UTP-3, Stages 2 and 4, and from Pile C57.

5.2 Pile UTP-4

The UTP-4 test started 27 days after construction. The response of the pile to the four loading stages was similar to that of Pile UTP-3. Figures 8 and 9 present the load-movement curves of the test stages for head-down tests on Pile UTP-4, Stages 1 and 3 and bidirectional-cell tests of Stages 2 and 4. For comparison, the downward load-movement of Pile UTP-3 is added to Figure 9. As shown, the toe stiffness of Pile UTP-3 is about twice that of Pile UTP-4, which difference is may be due to that the piles have different embedment lengths in the weathered bedrock (see Figure 5).

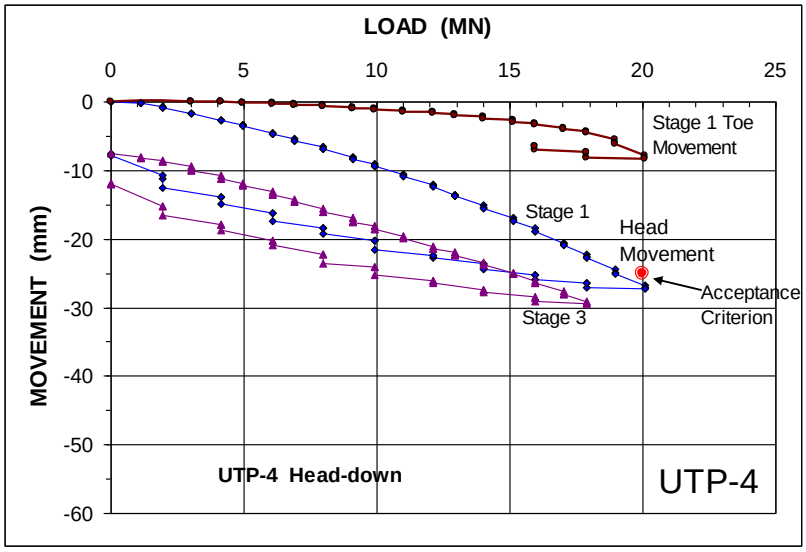

Fig. 8 Pile-head load-movement curves from Pile UTP-4; Stages 1 and 3

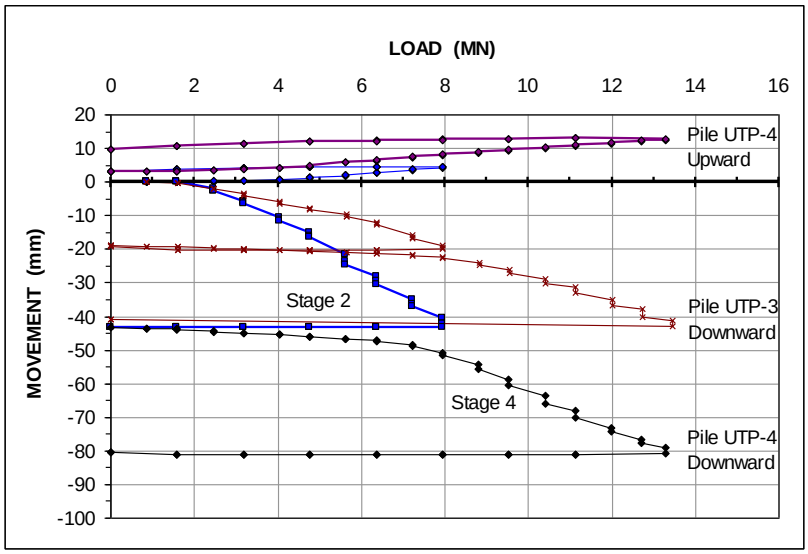

Fig. 9 Load-movement curves from Pile UTP-4; bidirectional-cell test, Stages 2 and 4with the downward curve from Pile UTP-3

5.3 Comments on Load-Movement Results

The toe stiffness response is an integral component of the pile head load-movement and it governs whether the test pile meets or fails the acceptance criterion. The differences in toe stiffness between the piles, Piles C57, UTP-3, and UTP-4 is thought due to difference in amount of debris present at the bottom of the piles at the time of concreting the pile. Despite the careful cleaning of the Piles UTP-3 and UTP-4 shafts, debris is believed to be present at the bottom of also these piles. The weathered granite contains, as mentioned, layers of silt and sand, which material is prone to enter the stabilizing slurry and, then, sink to the bottom of the shaft, where it is mixed with the concrete, resulting in a softened pile toe. When this occurs, it is very difficult to achieve a clean base. The toe stiffness response of Piles UTP-3 and UTP-4 is acceptable, and better results should probably not be expected when using a clean-out bucket for removing the debris. However, the cleaning out of the base of Pile C57 could have been more complete.

The direct measurement of the toe response is valuable for the assessment of expected settlement. However, load distribution assessment requires knowledge of the load transfer, which is where the analysis of the strain-gage data becomes important.

6. TEST RESULTS — STRAIN MEASUREMENTS AND LOAD

6.1 Pile UTP-3 Load-strain relations and shaft diameters

The strains induced by the loading of the pile head for Stages 1a and 1b, are shown in Figures 10A and 10B, respectively. The numbers above the curves denote each curve to its gage level. The two parallel hatch-marked lines indicate the slope of the records from Gage Level 13. The gages at Level 10 functioned erratically and are excluded. At Gage Level 1, only a single gage from of each pair, those at 12:00h position and 03:00h position functioned, which essentially made also that gage level inoperative.

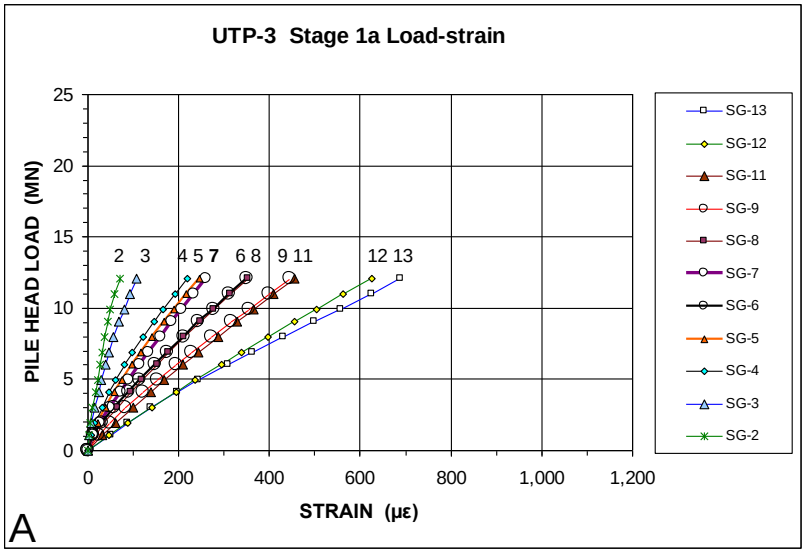

Fig. 10A Stage 1a Load-strain for each gage level as measured.

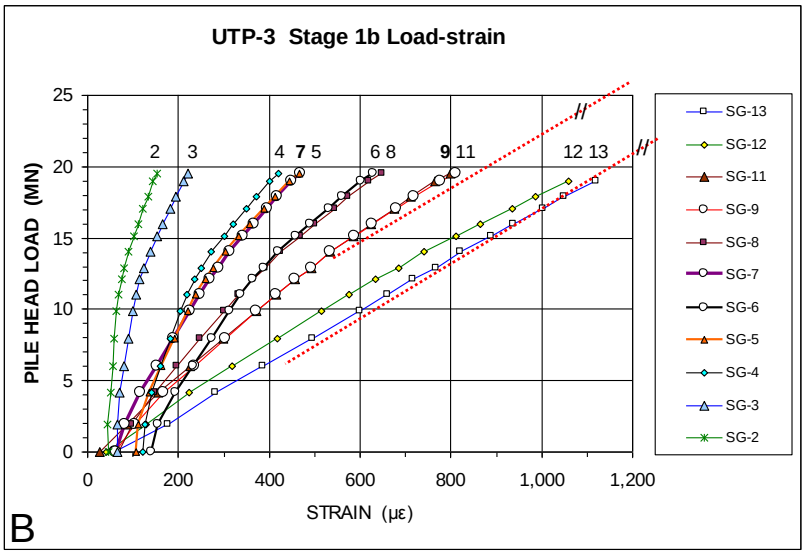

Fig. 10B Stage 1b Load-strain for each gage level as measured.

It would be expected that the curves be in sequence from left to right. That is, Gage Level 13, which is unaffected by shaft resistance should show the largest strains and progressively less strain should be shown by the gage levels deeper in the pile. As there is little shaft resistance present between Gage Levels 13 and 12, those curves should be close to each other with the other curves fanning out more the deeper down the pile the gage levels, because, not only does the unit shaft resistance get progressively larger with depth, the length of pile above the gage level where the soil is counteracting the applied load is getting progressively longer. Therefore, progressively less of the load reaches the deeper down gage levels. Where the shaft resistance is not fully mobilized, the curves should plot closer together.

It is assumed that the cross section at Gage Levels 13 and 12 are equal and correspond to the nominal pile diameter of 1.03 m, i.e., that of the outside diameter of the temporary casing. However, as shown, while the load-strain curves from Gage Level 13 and 12 respond as expected, the curves from Levels 9 and 8, 6, and 8 and 4, 5, and 7 are almost on top of each other. Moreover, the Level 7 curve is to the left of the Level 6 curve. These strain responses indicate that the shaft does not have a uniform cross section. For example, for the Level 7 curve to plot to the right of the Level 6 curve, as it should, the cross section of the pile at Gage Level 7 must be larger than that at Level 6. Moreover, the curve showing the load-strain for Gage Level 8 is unrealistically close to that of Level 6. In order to enable a single modulus to be used in the analysis, the pile diameters at Gage Levels 7, 8, and 9 were adjusted to 1,20 m, 1.14 m, and 1.10 m, respectively. Figures 11A - 11C show the load-strain curves after this adjustment. For clarity, the curves show only the strain values induced in the respective testing stage. The hatched parallel lines illustrate that the curves tend to be parallel toward the end of the test, when the shaft resistance has become fully mobilized.

The analysis of the strain data recorded from the test on Pile UTP-4 showed that UTP-4 Gage Levels 12 and 1 functioned erratically, and data from these levels were not used in the analysis. One gage pair at Level 1 was inoperative and the surviving pair gave data that suggested severe bending developing as the load increased in the

pile. The pile diameters at Gage Levels 7, 8, and 9, were again shown to need modification and they were adjusted to 1.13 m, 1.08 m, and 1.08 m, respectively. To save space, the corresponding, and quite similar, curves from Pile UTP-4 are not included in the paper.

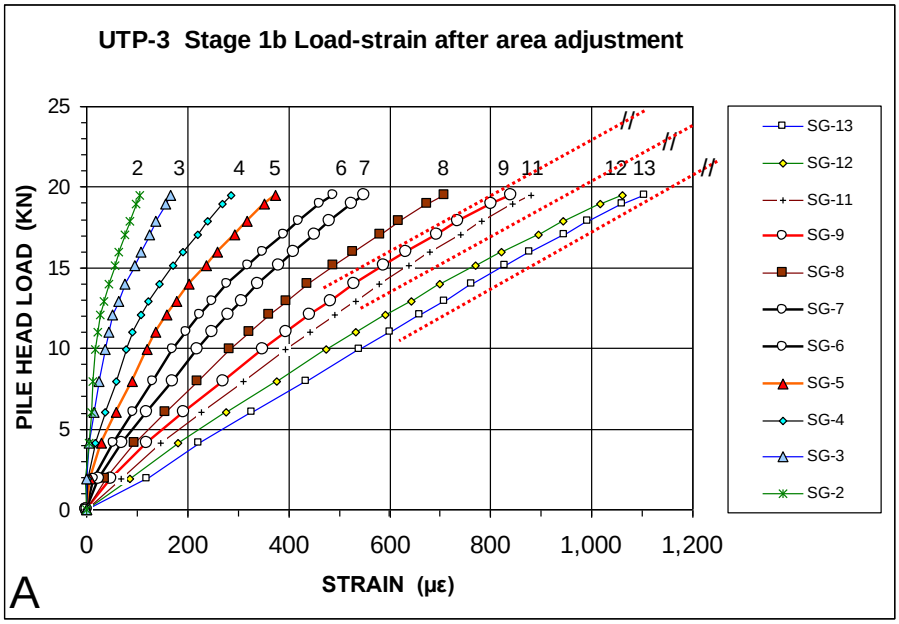

Fig. 11A Pile UTP-3 Stage 1b Load-strain for each gage level after area adjustment.

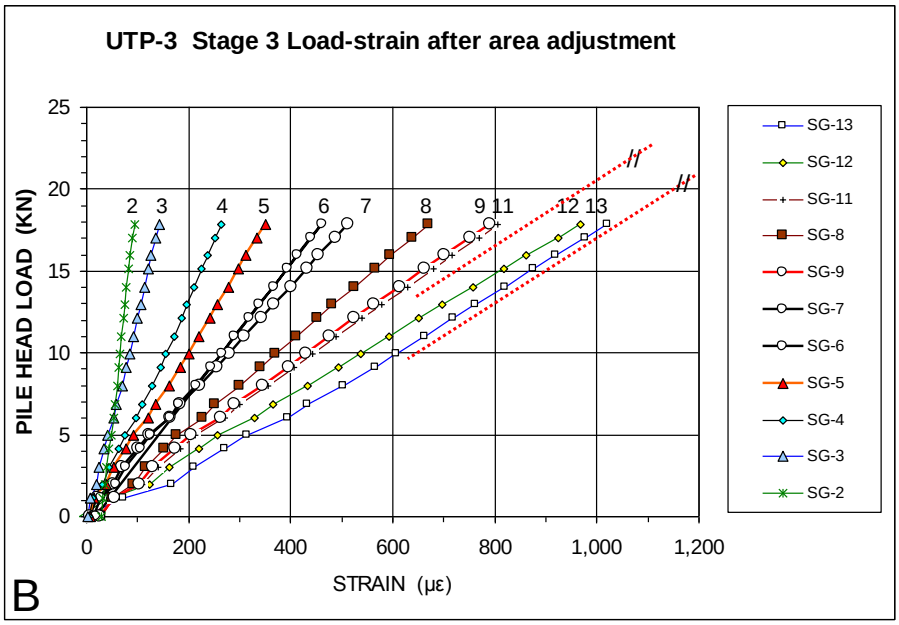

Fig. 11B Pile UTP-3 Stage 3. Load-strain for each gage level after area adjustment.

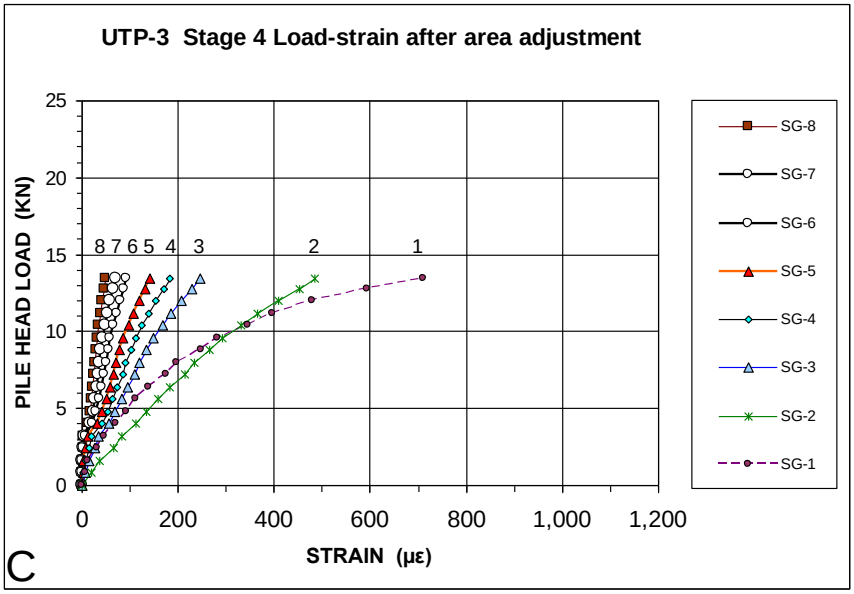

Fig. 11C Pile UTP-3 Stage 4. Load-strain for each gage level after area adjustment.

6.2 Tangent and secant modulus

In order to convert the strain values to load, it is necessary to know not only the pile cross section, but also the modulus of the concrete. Generally, the modulus of concrete ranges considerably for one project to another. Moreover, over the large strain range usually imposed in a static loading test, the concrete modulus is not a constant, but reduces with increasing strain. As indicated by Fellenius (1989, 2009), the actual modulus to use for the analysis of the strain data is best determined from a so-called "tangent modulus" or "tangent stiffness" plot, which presents the applied increment of load over the induced increment of strain, that is, the change of load over the change of strain, plotted versus the total strain. (The strain values used are those from the start of the Stage 1a test). For load increments after the shaft resistance has been fully mobilized, and provided that the shaft resistance is not strain softening or strain hardening, the values will plot along a slightly sloping line which defines the tangent modulus relation for the pile cross section. The tangent modulus is directly converted to secant modulus.

Figures 12A – 12D show the tangent modulus plots for Stages, 1a, 1b, 3, and 4. For Stage 2, the maximum load was not large enough to induce strain changes unaffected by shaft resistance, and, therefore, no tangent modulus line was apparent.

For calculating the loads represented by the secant modulus, the measured strains are multiplied with the nominal shaft diameter. The tangent modulus lines indicated in the figures correspond to a secant modulus, E_S (GPa), equal to 22 - 0.002 με. The similar analysis for Pile UTP-4 strain data showed an E_S (GPa) equal to 24 - 0.003 με.

The secant modulus values are low. Note, however, that the values are correlated to the 1.03 m nominal shaft diameter. If the actual diameter would be, say, 100 mm wider, then the evaluated moduli would be 20 % larger.

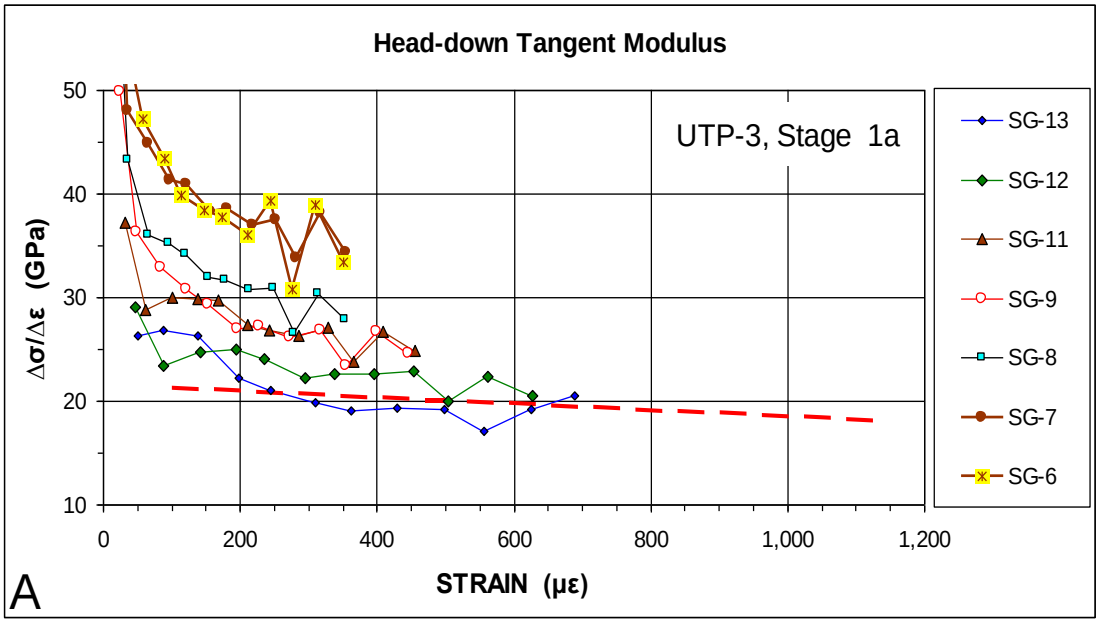

Fig. 12A Tangent modulus plot for Stage 1a

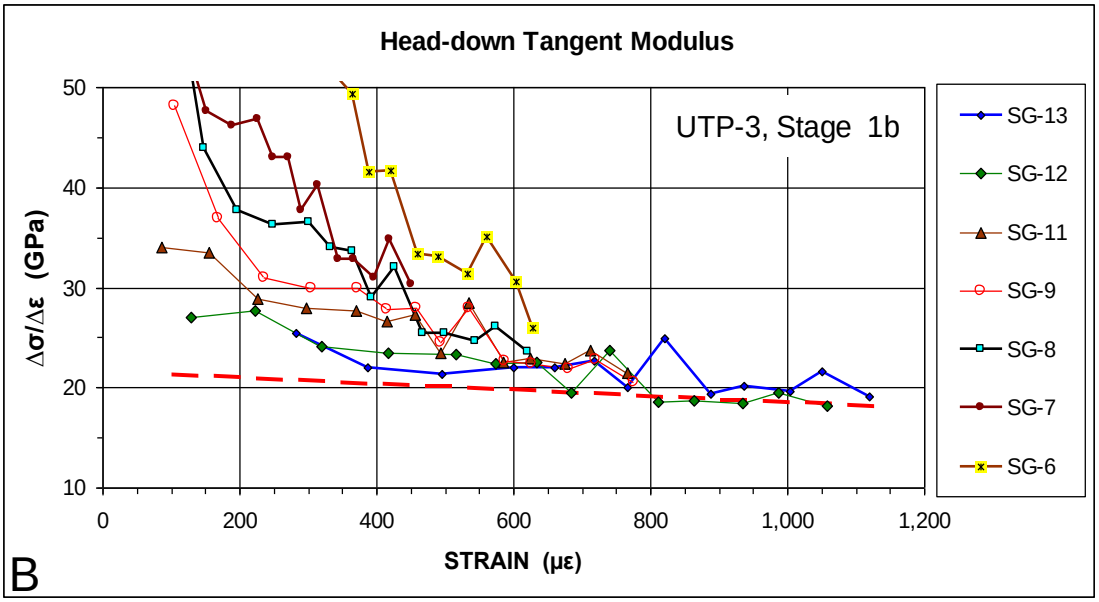

Fig. 12B Tangent modulus plot for Stage 1b

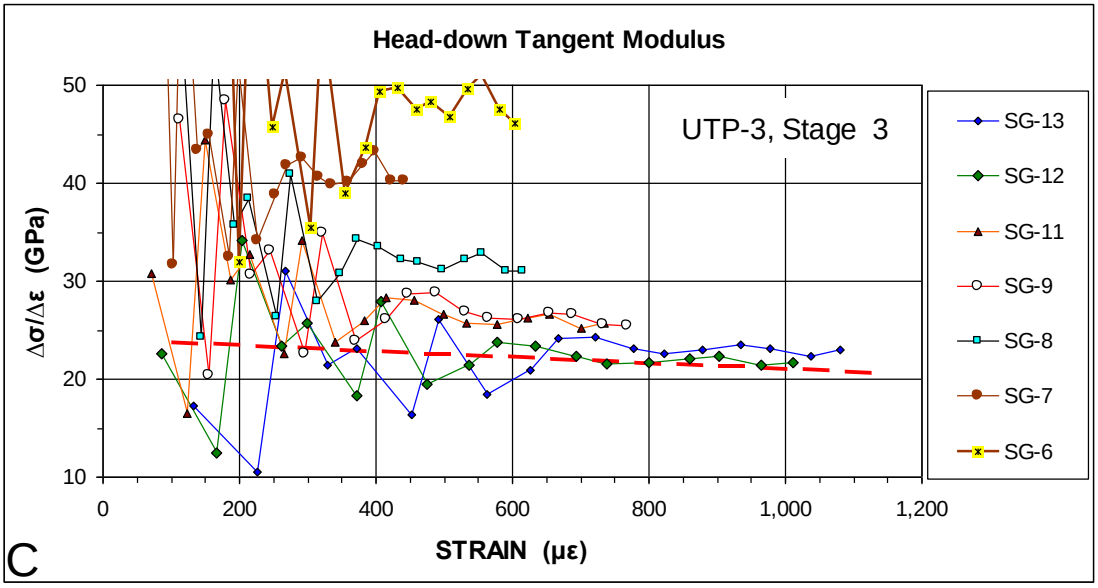

Fig. 12C Tangent modulus plot for Stage 3

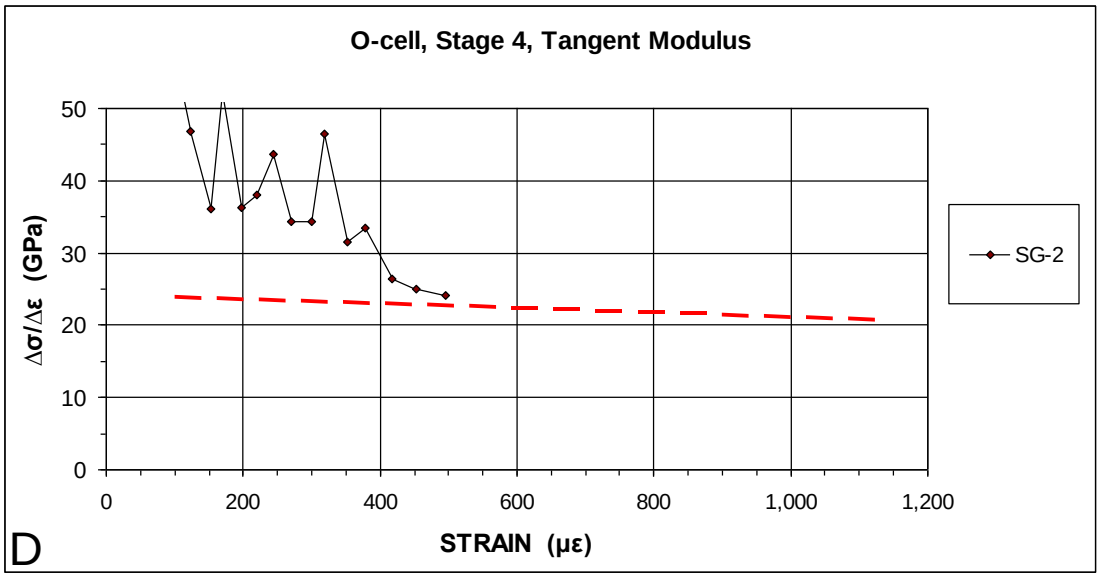

Fig. 12D Tangent modulus plot for Stage 4

6.3 Load distribution

The strains induced from the start of Stage 1a were combined with the secant modulus relation and the nominal shaft diameter to determine the load represented by the strain values. The strain values for Gage Levels 7, 8, and 9 were proportioned to the respective adjusted shaft diameter. The calculated load distributions for Stages 1b, 2, 3, and 4 are shown in Figures 13A – 13D.

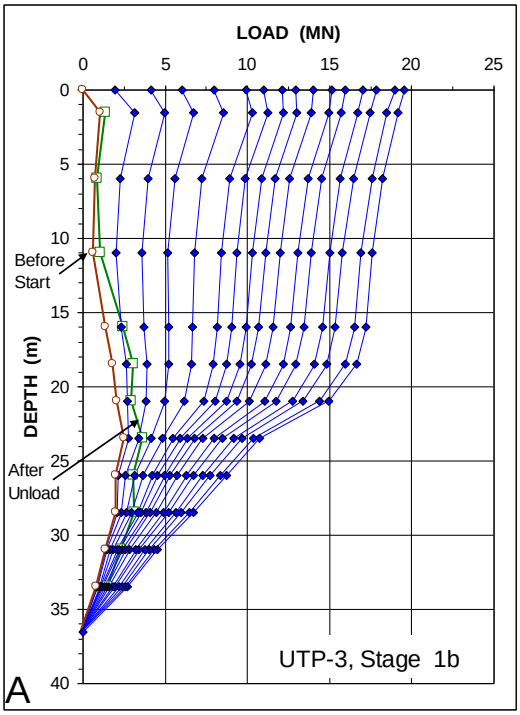

Fig. 13A Load distribution for Pile UTP-3, Stage 1b

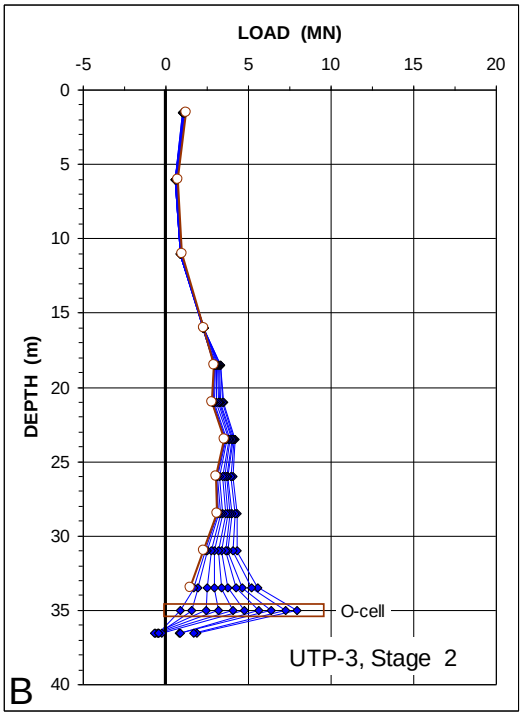

Fig. 13B Load distribution for Pile UTP-3, Stage 2

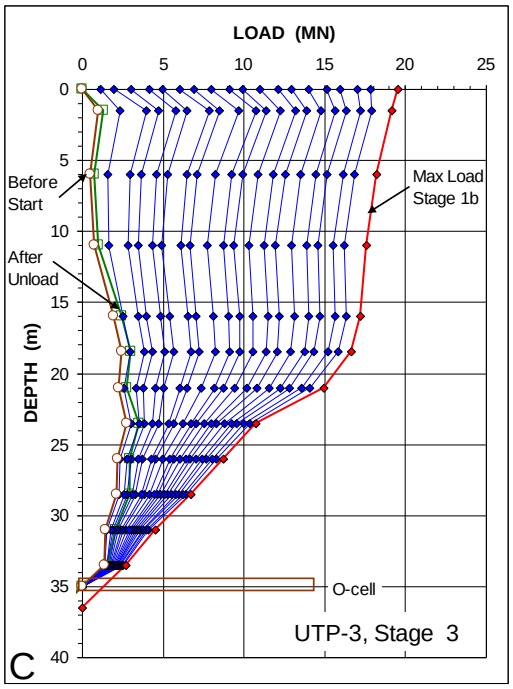

Fig. 13C Load distribution for Pile UTP-3, Stage 3

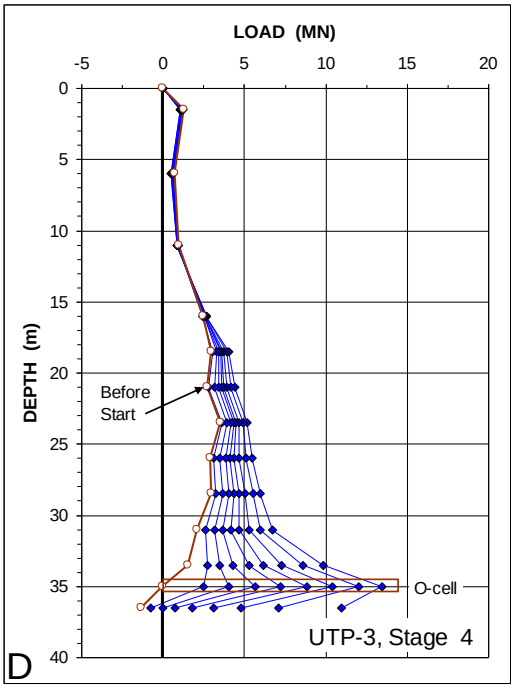

Fig. 13D Load distribution for Pile UTP-3, Stage 4

For all distributions, each preceding test introduced additional load in the pile after unloading. Gage Level 1 indicated that the "tack breaking" resulted in a small release of locked-in load in the pile. Because of the low stiffness of the pile toe, the 13.5 MN maximum Stage 4 cell load could only activate the shaft resistance along a distance of about 8 m to 10 m up from the cell. No appreciable load reached beyond 20 m up from the cell. In contrast, the 19.5 MN maximum head-down load did mobilize full shaft resistance down to at least about 25 m.

To compare the load distribution determined in the cell (Stage 4) test to that of the conventional head-down test (Stage 1b), the load distribution above the cell, which consists of accumulated negative direction shaft resistance, needs to be "flipped" over to its mirrored distribution of positive shaft resistance along the entire length of the pile, as shown in Figure 14. The so-determined load distribution can now be compared to the head-down distributions, Stages 1 and 3.

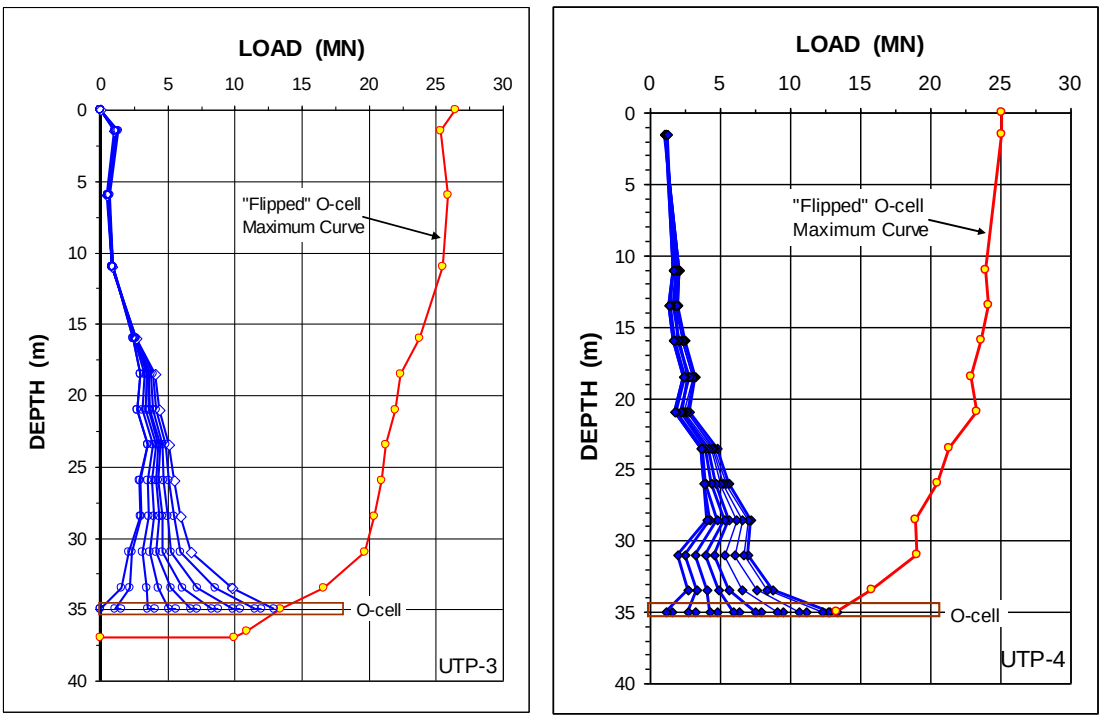

Fig. 14 Load distributions for Piles UTP-3 and UTP-4 as measured and as "flipped"

Figure 15A shows the head-down and "flipped cell distributions for Piles UTP-3. Down to a depth of about 30 m, the head-down tests gave the largest shaft resistance, whereas below this depth, the shaft resistance from the cell is the largest. The actual tested shaft resistance is therefore the bidirectional-cell curve up to this depth and the head-down curve, moved over, to the rest of the way to the pile head. Thus, combining the results of the two test methods a tested maximum head-down test load of 38 MN is obtained. This value is about twice the maximum load applied to the pile head in the head-down tests and about three times the maximum load in the tests.

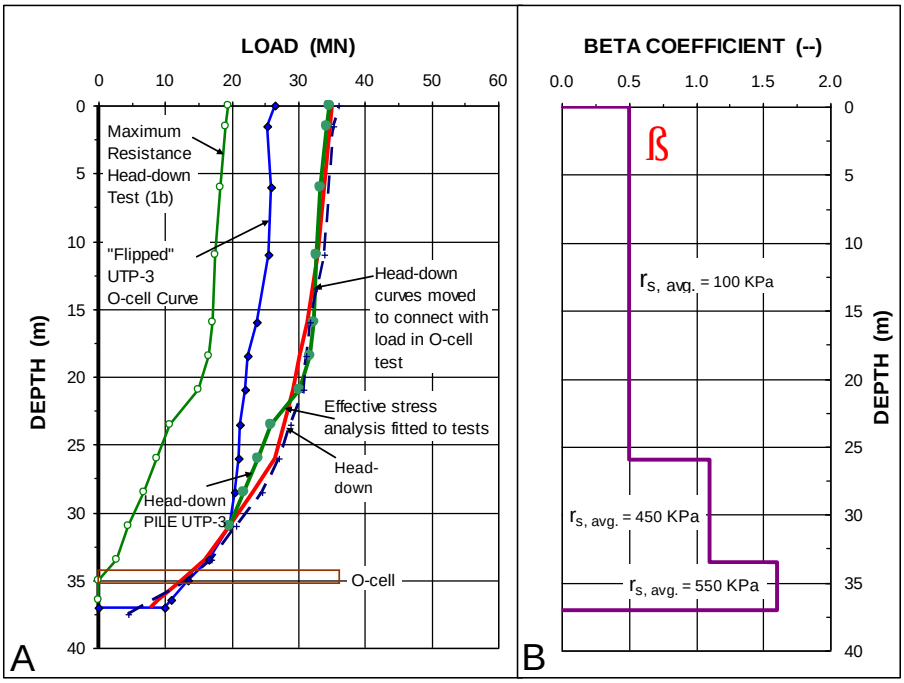

Fig. 15 Distributions of load and Beta-coefficient

The Pile UTP-4 results are almost the same as the Pile UTP-3 results. While the shaft resistance determined for the two test piles between the depths of 17 m and 34 m show some local variation, the total value is nearly the same for the two test piles. However, for Pile UTP-3 the shaft resistance over this length is obtained in the residual soil, whereas for Pile UTP-4, it is in the fractured granite (the weathered bedrock).

It is always interesting to correlate shaft resistance obtained from analysis of results of a loading test to the effective overburden stress. Figure 15B shows the distribution of beta-coefficients (ratio between unit shaft resistance and effective overburden stress) determined from fitting the UTP-3 load distribution to an effective stress analysis. Usually, the shaft resistance of a bored pile constructed in bedrock, even in fractured bedrock, is thought not to correlate to the effective overburden stress. Therefore, the fact that a fit was possible and that beta-values increase reasonably with the soil change over depth does not necessarily mean that the shaft resistance is governed by effective stress in the weathered soil and rock at the site. Figure 15B also shows the average values of unit shaft resistance, $r_{s,\ avg}$, over the same length of pile is constant where the fitted beta-coefficient increases.

Pile capacity is often correlated to the results of a CPT or CPTU sounding (Eslami and Fellenius 1997). The two soundings results shown in Fig. 1 were used to calculate the shaft resistance for an 11.0 m long pile similar to the test piles according to four methods Eslami-Fellenius (Eslami and Fellenius 1997), Dutch (DeRuiter and Beringen 1979), LCPC (Bustamante and Gianeselli 1982, and Schmertmann (1978). The latter three methods are based on the CPT, that is, they do not include the correction for pore pressure on the cone shoulder. Table 1 shows the shaft resistance determined for the pile length between 3.5 m prebored depth and 11 m depth and the shaft resistance along the same length calculated using the two CPTU soundings according to the four mentioned methods.

TABLE 1 Shaft resistance from test and from four analyses of cone sounding data

Measured in Test (kN)	Cone Sounding (ID)	Eslami-Fellenius (kN)	Dutch Method (kN)	LCPC Method (kN)	Schmertmann Method (kN)
700	CPTU-01	780	750	190	220
700	CPTU-02	1,030	1,800	610	380

The calculated values differ between the methods and between the two cone soundings. (As shown in Table. 1, the cone soundings themselves are quite different). The results of the CPT/CPTu calculations are mainly offered to demonstrate that using cone data in an actual engineering project is great for determining soil layering, but one needs to be cautious in applying the results numerically to resistance distributions.

7. CONCLUSIONS

1. Although the tests were affected by low pile toe stiffness and excessive upward movement of the reaction kentledge beams, the test result provided the desired information needed for proceeding with project foundation design.
2. The head-down tests showed that the two carefully constructed piles, Piles UTP-3 and UTP-4, just about satisfied the acceptance criterion. The acceptance criterion says very little about the test pile, but is presumably a limit referencing the requirements of the structure supported on the piles. Most of the measured pile head movements were due to pile compression for the load. The pile toe movements were small, 3 mm and 6 mm, only, for Piles UTP-3 and UTP-4, respectively.
3. The bidirectional-cell test showed that the pile toe response was less stiff than expected. This is thought due to presence of soil debris at the bottom of the shaft when concreting the pile despite the careful cleaning of the base. However, due to the greater care in cleaning the pile base of Piles UTP-3 and UTP-4 before concreting, the toe response was stiffer than that found for the first two test piles and, therefore, satisfactory. In order to ensure a stiffer pile toe, other means than a cleaning bucket for cleaning out the pile shaft bottom would be necessary.

4. The evaluation of the strain-gage data showed that the secant modulus, E_s (GPa), of the pile material was a function of the induced strain and equal to $22.0 - 0.002\mu\varepsilon$ and $24.0 - 0.003\mu\varepsilon$, for Piles UTP-3 and UTP-4, respectively.
5. The load distribution for the two test piles was very similar and could be fitted to a reasonably smooth distribution of beta-coefficient as well as average unit shaft resistance.
6. Combining the two test methods, the results can be considered equal to a head-down test with an applied maximum load of 38 MN, which is smaller than the ultimate resistance value (total capacity).

ACKNOWLEDGEMENT

All static loading tests were performed by LoadTest Asia Inc., Singapore. The authors are grateful to the engineers for the project, KTP Consultants Pte. Ltd., Singapore, for permission to publish the tests results.

REFERENCES

Bustamante, M. and Gianeselli, L., 1982. "Pile bearing capacity predictions by means of static penetrometer, CPT." Proceedings of the Second European Symposium on Penetration Testing, ESOPT II, Amsterdam, May 24 27, A.A. Balkema, Vol. 2, pp. 493-500.

DeRuiter, J. and Beringen, F.L., 1979. "Pile foundation for large North Sea structures." Marine Geotechnology, (3)3 267-314.

Eslami, A. and Fellenius, B.H., 1997. "Pile capacity by direct CPT and CPTu methods applied to 102 case histories." Canadian Geotechnical Journal 34(6) 886-904.

Fellenius, B.H., 1989. "Tangent modulus of piles determined from strain data." American Society of Civil Engineers, ASCE, Geotechnical Engineering Division, the 1989 Foundation Congress, F.H. Kulhawy, Editor, Vol. 1, pp. 500-510.

Fellenius, B.H., 2000. "The O-Cell—A brief introduction to an innovative engineering tool." Väg- och Vattenbyggaren 47(4) 11-14.

Fellenius, B.H., 2009. "Basics of foundation design, a text book." Revised Electronic Edition, [www.Fellenius.net], 330 p.

Osterberg, J.O., 1998. "The Osterberg load test method for drilled shaft and driven piles. The first ten years." Great Lakes Area Geotechnical Conference. Seventh International Conference and Exhibition on Piling and Deep Foundations, Deep Foundation Institute, Vienna, Austria, June 15-17, 1998, 17 p.

Schmertmann, J.H., 1978. "Guidelines for cone test, performance, and design." Federal Highway Administration, Report FHWA TS 78209, Washington, 145 p.

Zao, J., Broms, B.B., Zhou, Y., and Choa, V., 1994. "A study of the weathering of the Bukit Timah Granite." Part A: Review, field observations, and geophysical survey. Bulletin of the International Association of Engineering Geology, Vol. 49, pp. 97-106.